

Short-wavelength far-infrared laser cavity yielding new laser emissions in CD₃OH

M. Jackson^{1,*}, E.M. Telles², M.D. Allen³, K.M. Evenson³

¹Department of Physics, University of Wisconsin–La Crosse, La Crosse, WI 54601, USA

²Instituto de Física Gleb Wataghin, Universidade Estadual de Campinas – UNICAMP, 13.083-970, Campinas, S.P., Brasil

³Time and Frequency Division, 847.00, National Institute of Standards and Technology, 325 Broadway, Boulder, CO 80303, USA

Received: 26 October 2000/Published online: 7 February 2001 – © U.S.-Government 2000/Springer-Verlag 2001

Abstract. A significantly improved far-infrared laser has been used to generate optically pumped laser emissions from 26 to 150 μm for CD₃OH. Using an *X*–*V*-pumping geometry, several new laser emissions have been found for CD₃OH. In addition, an increase in power, by factors from 10 to 1000, for many of the previously known shorter-wavelength laser lines, below 100 μm , has been observed. Frequency measurements for several lines have also been performed and have been reported to a fractional uncertainty up to $\pm 2 \times 10^{-7}$, permitting the spectroscopic assignment of the laser transition. One of the frequency-measured lines, 44.256 μm observed using the 10R34 pump, has confirmed the assignment of the previously reported FIR emission $(n, K; J) = (1, 7; 20) \rightarrow (0, 8; 20)A$ in the ground vibrational state.

PACS: 42.60.By; 42.60.Da; 42.62.Fi

Following the initial observation of far-infrared (FIR) laser emissions from methanol (CH₃OH) by Chang et al. [1], methanol and its isotopes have produced more than 2000 FIR laser lines when optically pumped by cw and pulsed CO₂ lasers [2, 3]. CD₃OH alone contributes more than 400 laser lines in the wavelength range 21.7–3030.0 μm [2–4]. The richness of FIR emissions is principally due to the excellent overlap between the CD₃-deformation region (1068.2 cm^{-1}) and the C–O vibrational band (984.4 cm^{-1}) with the 9- and 10- μm CO₂ laser bands, respectively [5, 6].

In this paper, we report the discovery of new optically pumped FIR laser emissions from CD₃OH. Using a new FIR cavity and pumping scheme, designed for wavelengths below 100 μm , substantial increases in output power for many previously observed emissions [7–15] have been found. Frequency measurements on several new lines have also been performed.

*Corresponding author.

(Fax: +1-608-785-8403, E-mail: jackson.mic2@uwlax.edu)

1 Experimental details

The experimental setup for the optically pumped molecular laser (OPML) system is partially shown in Fig. 1. The CO₂ pump laser is 2-m long and includes a partially ribbed cavity surrounded by a water-cooled jacket. The Pyrex-glass tube has an inner diameter of 18 mm and contains five equally spaced glass ribs whose inner diameters increase from 16.5 to 17.5 mm. By introducing glass ribs into the laser cavity many wall-bounce modes are eliminated, thereby forcing an open-structure mode and increasing the effective resolution of the grating [16]. The laser uses the zeroth-order output coupling from a 150-line/mm grating with 3% output coupling in zero order. The CO₂ laser is capable of producing ≈ 275 lines, including lines on the regular-, hot- and sequence-band emissions. A high-reflectivity gold-coated 20-m-radius mirror is used on the other end. Both the 9- and 10- μm branches exhibit high-*J* lines out to 9R(58), 9P(60), 10R(58) and 10P(60). Regular laser lines reach powers up to 30 W with the hot- and sequence-band emissions reaching 10 W [17].

The CO₂ laser radiation is focused into the FIR cavity with a 12-m-radius-of-curvature gold-coated concave mirror, externally mounted on the far (fixed-mirror) end of the

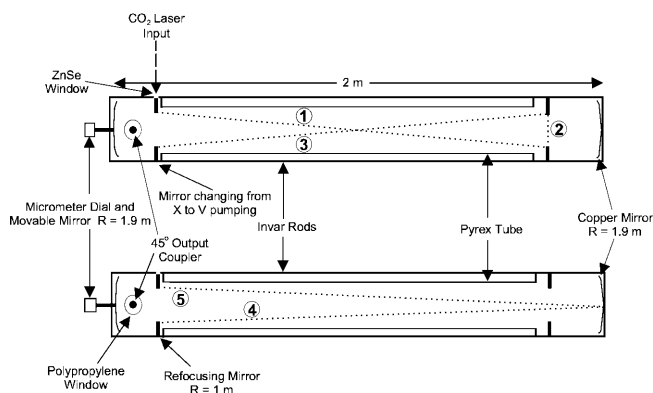


Fig. 1. Side view of the optically pumped molecular laser system

cavity at approximately 2 m from the 20-mm-diameter ZnSe window. A flat gold-coated mirror then reflects the CO₂ beam into the FIR cavity and to the X-V mirror system. This mirror system, shown in Fig. 1, uses three 19-mm-diameter copper mirrors along with one of the FIR cavity mirrors. Each of the four copper mirrors extends about 20 mm into the FIR cavity and transmits $\approx 99\%$ of the 118.8- μm line of CH₃OH through the FIR window. The advantage to this is that many of the longer-wavelength lines are suppressed, thereby allowing some of the shorter wavelengths to emerge.

In the pumping geometry shown in Fig. 1, a 45° mirror first reflects the beam across the vertical plane of the cavity (path 1). At the other end, two identical 45° mirrors are used to redirect the CO₂ beam to the bottom of the input chamber (paths 2 and 3, which complete the X-portion of the pumping scheme). A gold-plated copper mirror with a 1-m radius of curvature then reflects the CO₂ beam to the main FIR cavity mirror (path 4). This curvature was chosen so that the beam diameter would be slightly larger than a 40- μm Gaussian beam waist. Finally the CO₂ beam is reflected from the FIR mirror, to the input 45° mirror and out of the FIR system (path 5, which completes the V-portion of the pumping scheme). One advantage to this type of pumping design over simpler configurations, such as the V-pumping geometry, is that the additional passes allow more of the gain medium to be pumped. In addition, with this design it was rather straightforward to introduce a slight horizontal angle into the CO₂ beam so that the exiting radiation does not retrace its entire path and re-enter the CO₂ cavity. The elimination of feedback was a significant improvement over previous designs. Although several other designs were used, including having the X-pump in the vertical plane with the V-pump in the horizontal plane, no increase in efficiency or output power was then observed.

The FIR cavity is about 2-m long and utilizes a nearly confocal mirror system, consisting of two 1.9-m radius of curvature concave gold-coated copper mirrors with a 50-mm diameter. Four invar rods connect the endplates holding the FIR mirrors and the 2-m-long Pyrex-glass tube with a 59-mm inner diameter. One copper mirror is attached to a micrometer and is moved to tune the cavity into resonance with the FIR laser modes. A 6-mm-diameter 45° copper mirror is situated on the side of the cavity and couples the FIR power out horizontally through a polypropylene window, 25-mil thick. One varies the output coupling by moving the 45° copper mirror radially into and out of the cavity mode. The generated FIR radiation is focused by an off-axis parabolic mirror onto a pyroelectric detector or metal-insulator-metal (MIM) point-contact diode.

Wavelength measurements of the FIR radiation were made by tuning the Fabry-Perot cavity with the movable end mirror and measuring the mirror displacement for 20 wavelengths of that laser mode. The value thus obtained is accurate to within $\pm 0.5 \mu\text{m}$. Due to the intense number of laser lines observed in several scans, some wavelength measurements were made with 10 and 5 wavelengths; these are denoted accordingly in Table 1. A set of absorbing filters calibrated with wavelength discriminate against CO₂ laser radiation from reaching the detector, as well as helping distinguish different FIR wavelengths. The relative polarizations of the laser

lines were measured with a multi-Brewster-angle polarization selector.

The frequencies of optically pumped FIR laser lines were measured by mixing the unknown FIR frequency with two CO₂ laser frequencies and microwaves in a MIM diode. The frequency standards were synthesized from the difference between two CO₂ laser frequencies stabilized by locking each directly to a saturation dip in the 4.3- μm CO₂ fluorescence signal from an external reference cell [18]. The pair was chosen to be close to the unknown FIR frequency calculated from its wavelength measurement. A microwave signal ($\nu_{\mu\text{wave}}$) from a synthesized signal generator can also be mixed on the MIM diode if the CO₂ difference is outside the band of a spectrum analyzer.

The signal from the MIM diode is pre-amplified and then observed on the spectrum analyzer to determine the beat note (ν_{beat}) at the frequency given by the equation:

$$\nu_{\text{FIR}} = |n_1 \nu_{\text{CO}_2(\text{I})} - n_2 \nu_{\text{CO}_2(\text{II})}| \pm m \nu_{\mu\text{wave}} \pm \nu_{\text{beat}} \quad (1)$$

The integers n_1 , n_2 and m correspond to their respective harmonics generated in the MIM diode. The (+) or (−) signs and the values of n_1 , n_2 and m are determined experimentally by tuning the FIR laser frequency and the microwave frequency and observing the beat-note shift on the spectrum analyzer.

The estimated one-sigma uncertainty of frequency measurements is, at best, on the order $\Delta\nu/\nu = 2 \times 10^{-7}$. It is due mainly to the uncertainty in the setting of the FIR laser cavity to the center of its gain curve. For minimizing this uncertainty, we tuned the FIR laser across its gain curve and observed the change to the beat note on the spectrum analyzer using a peak-hold feature. The value of this frequency is calculated from the average of at least ten different measurements.

2 Results

Table 1 and 2 present the wavelength listing of the FIR laser emissions observed in this investigation for new and previously known lines, respectively. The polarization relative to the pump laser, operating pressure and relative intensity are listed when available. The intensity of the FIR output is given as a listing ranging from very very strong (VVS) to very weak (VW). In this work, a VVS line is expected to provide a power greater than 10 mW¹ when all the parameters (pump laser, FIR resonator, coupling mirror, pressure, etc.) have been optimized. Optimization of the FIR cavity was done to the best of our ability, but in no way should be taken as an absolute measure since the relative intensities of FIR emissions are subject to the experimental apparatus used [19]. The lines labeled with VS, S, M, W and VW have ranges in power from 10–1 mW, 1–0.1 mW, 0.1–0.01 mW, 0.01–0.001 mW and below 1 μW , respectively.

In most situations, the relative intensity and polarization were measured with the pyroelectric detector. The disadvantage of using the MIM in these situations is that it tends to favor one polarization over another. As a result, some lines appearing as very weak parallel lines may actually appear as medium perpendicular lines. Only one new line, 48.4 μm

¹ The 118.8- μm line of CH₃OH is considered to be VVS

Table 1. New optically pumped laser emissions from CD₃OH

Pump	Wavelength (μm)	Rel. pol.	Pressure (mTorr)	Rel. intensity
9R28	48.4 ^c		202	M
	50.6 ^{b,d}		255	S
9P08	39.9 ^c		190	M
9P28	64.045 ^{a,f}		200	M
9P32	46.4 ^c		70	M
9P34	28.4 ^b		160	W
9P40	32.4 ^c	⊥	180	W
9P56	69.8 ^c	⊥	110	M
10R48	26.3 ^b	⊥	280	W
10R36	67.4 ^c	⊥	270	VS
10R34	44.256 ^{b,f}		180	M
	127.6 ^{b,e}	⊥	310	S
10R32	111.6 ^a	⊥	400	M
10R08	41.3 ^a		160	S
10P24	38.0 ^c	⊥	188	W
	130.0 ^{a,e}		150	M
10P32	80.1 ^c		154	M
10P36	68.1 ^a	⊥	330	S

^a Wavelength measured using $40\lambda/2$

^b Wavelength measured using $20\lambda/2$

^c Wavelength measured using $10\lambda/2$

^d Observed at the same offset

^e Observed with a slightly different offset

^f Calculated from frequency measurement, Table 3

observed with the 9R28 pump, was found with the MIM detector.

In addition to the improved detection of previously known lines, Table 2 also lists ten lines reported with new polarizations, as well as two lines observed with a polarization different from the one previously reported. The X-V-pumping geometry has been found to be so efficient that the polarization of the FIR emission is determined, in some cases, by the pump polarization. The previously observed lines are reported using the wavelengths given in the review papers by Zerbetto and Vasconcellos [2] and Pereira et al. [3], unless otherwise noted. The reported wavelengths were within the uncertainty of our measurements, $\pm 0.5 \mu\text{m}$.

Table 3 gives the frequency measurements of optically pumped CD₃OH. All frequency measurements are new with the exception of the 55.5- μm wavelength found with the 10R20 pump. This frequency did differ by 4.5 MHz from the previously reported value [15]². Due to the different type of FIR cavity and pumping geometry used, in addition to the other experimental conditions, a change of a few MHz is not completely unexpected [17, 20, 21]. This includes the possibility that absorption of the CO₂ beam by the FIR medium may have only occurred for molecules moving in one direction, resulting in a slight shift in the center frequency of the FIR emission. This effect would be enhanced if the CO₂ laser was operated on the edge of its gain curve.

Finally, Moraes [22] recently predicted the assignment of several lines associated with a closed combination loop using the 10R34 CO₂ pump. Two of these lines were predicted to be 199.1082 cm^{-1} ($50.224 \mu\text{m}$) and 225.1929 cm^{-1} ($44.406 \mu\text{m}$), with the latter assigned to the FIR emission

² As a check, this frequency was also measured using a 1.5-m-long CO₂ laser cavity with a 133-line/mm grating, coupling 10% in the zeroth order. The laser frequency was reproducible to within $\pm 0.8 \text{ MHz}$

Table 2. Improvement in previously observed laser emissions from optically pumped CD₃OH

Pump	Wavelength (μm)	Rel. pol.	Pressure (mTorr)	Rel. intensity	
				New	Old
9R34	53.82	⊥	240	VVS	M, VS
9R28	42.6 \pm 0.2	^c	198, 288	VS	S
	44.3 \pm 0.2	⊥ ^c	288	S	S
	55.6 \pm 0.1	⊥	288	VS	
9R06	56.538	⊥	180	VS	M, S
	68.45 \pm 0.1		160, 190	VS	W
9P08	44.7 \pm 0.1	⊥	170, 190	S	W
9P28	47.1 \pm 0.2	^c	190	S	S
	54.1 \pm 0.3	⊥ ^c	190	VS	S
9P30	30.7 \pm 0.2	^c	100	S	M
9P38	42.5	^c	190	M	M
	42.92 \pm 0.1		198	S	W, M
9P56	129.2 ^a		110, 190	VS	M
10R56	51.478 ^b		144	M	W
10R48	43.7 \pm 0.1		280	M	W
10R46	68.8 \pm 0.1	⊥	288	VS	W
10R38	51.40 \pm 0.05		270	S	W
10R36	68.21 \pm 0.07	^c	208	S	VW
10R34	34.1 \pm 0.2	⊥ ^c	85	VS	S
	37.25 \pm 0.04		120, 170	VS	M
	42.5	⊥ ^d	218	VVS	M
	86.742	⊥	200	VS	M
	128.7 \pm 0.6		188	S	VW
	191.356		310	VS	M
10R32	83.9 \pm 0.1		244	VS	M, S
	131.563	⊥	244	VS	M, S
10R30	67.479		128, 178	VS	M
10R24	49.973 ^b	^c	196	VS	M
10R20	55.3 \pm 0.1	^d	260	S	W
10R18	41.355	⊥	155	VVS	S, VS
	43.697		182	VVS	VS
10R16	81.557		188, 250	VS	W, M
10R14	107.2 \pm 0.1		134	VS	M
10R08	41.5 \pm 0.1	⊥	120	VS	M
	45.0 \pm 0.1		95	VS	M, S
10P10	108.668		176	S	W, M
10P18	144.118		218	VS	M, S
10P20	89.668 ^b		210	S	M
10P22	34.8 \pm 0.1		210	VS	M
	40.289 ^b	⊥	210	S	W, M
10P24	47.2	⊥	188	S	M
10P32	105.2	^c	130	S	M
10P48	76.93 \pm 0.1		155	M	W

^a From [15]

^b From K.M. Evenson, private communication

^c New polarization

^d Polarization differs from value previously reported

Table 3. New frequency-measured laser emissions from optically pumped CD₃OH

Pump	Frequency ^a (MHz)	Wavelength ^b (μm)	Wavenumber ^b (cm^{-1})
9P28	4680996.9 \pm 0.2	64.045	156.1412
9P56	2323198.8 \pm 0.9	129.043	77.4936
10R34	6774066.2 \pm 0.3	44.256	225.9585
10R24	4873764.7 \pm 0.9	61.512	162.5713
10R16	3463216.5 \pm 0.5	86.565	115.5205
10R20	5413024.0 \pm 0.8 ^c	55.384	180.5591

^a All lines were observed to have parallel (||) polarizations

^b Calculated using $1 \text{ cm}^{-1} = 29979.2458 \text{ MHz}$

^c Previously measured as 5413019.5 MHz [15]

$(n, K; J) = (1, 7; 20) \rightarrow (0, 8; 20)A$ in the ground vibrational state. Although the measurement of the first line was close to the predicted value, 199.60 cm^{-1} , the second measurement was further off, 235.29 cm^{-1} ($42.5 \mu\text{m}$). Assignment of the transition to this line was reasonable however, since no frequency measurements were available and no other wavelengths were known at the time. We propose that our newly discovered frequency-measured line 225.9585 cm^{-1} ($44.256 \mu\text{m}$), observed with the 10R34 CO₂ pump, will serve as a better fit for the assignment of this transition and for inclusion in this particular closed combination loop.

3 Discussion and conclusions

We report 18 new lines of CD₃OH and 5 new frequency measurements from this molecule. For each new line, the wavelength, polarization relative to the pump laser, FIR cavity pressure and the observed relative intensity are given. Since most of the new lines have wavelengths below $100 \mu\text{m}$ they will be useful for filling the gaps currently existing in this portion of the FIR region.

In this work, we have also demonstrated the effectiveness of the X–V-pumping geometry on short-wavelength emissions. In addition to the new lines discovered, over thirty previously observed lines were found to increase in power by factors of 10 to 100 with several increasing by a factor of 1000. Although designed for shorter FIR wavelengths, lines up to $253.72 \mu\text{m}$ were observed.

Finally, the lines reported in this paper will be useful for future assignments of FIR laser emissions from this molecule by calculation of combination loops from high-resolution Fourier-transform data [23]. This is illustrated by the confirmation of the FIR assignment $(n, K; J) = (1, 7; 20) \rightarrow (0, 8; 20)A$ in the ground vibrational state [22]. The new frequency measurements will also be useful in the assignments of lines involved in an IR–FIR laser system. In addition, the new pumping geometry will further aid in the discovery of new short-wavelength emissions as well as provide a source of short-wavelength FIR emissions with sufficient intensity to be used in spectroscopic studies, such as laser magnetic resonance.

Acknowledgements. The authors are pleased to acknowledge the following programs for financial support: the National Science Foundation

(CRIF – #9982001), the Wisconsin Space Grant Consortium, the College of Science and Allied Health, University of Wisconsin–La Crosse (M.J.) and FAPESP, São Paulo, Brazil 97/7445-3 (E.M.T.).

References

1. T.Y. Chang, T.J. Bridges, E.G. Burkhard: *Appl. Phys. Lett.* **17**, 249 (1970)
2. S.C. Zerbetto, E.C.C. Vasconcellos: *Int. J. Infrared Millimeter Waves* **15**, 889 (1994)
3. D. Pereira, J.C.S. Moraes, E.M. Telles, A. Scalabrin, F. Strumia, A. Moretti, G. Carelli, C.A. Massa: *Int. J. Infrared Millimeter Waves* **15**, 1 (1994)
4. N.G. Douglas: *Millimetre and Submillimetre Wavelength Lasers: A Handbook of CW Measurements* (Springer, New York 1989)
5. I. Mukhopadhyay, M. Mollabashi, R.M. Lees: *J. Opt. Soc. Am. B* **14**, 2227 (1997)
6. F.C. Cruz, A. Scalabrin, D. Pereira, P.A.M. Vazquez, Y. Hase, F. Strumia: *J. Mol. Spectrosc.* **156**, 22 (1992)
7. E.J. Danielewicz, C.O. Weiss: *IEEE J. Quantum Electron.* **QE-14**, 458 (1978)
8. T. Yoshida, T. Yoshihara, K. Sakai, S. Fujita: *Infrared Phys.* **22**, 293 (1982)
9. H. Sigg, H.J.A. Bluysen, P. Wyder: *IEEE J. Quantum Electron.* **QE-20**, 616 (1984)
10. D. Pereira, C.A. Ferrari, A. Scalabrin: *Int. J. Infrared Millimeter Waves* **7**, 1241 (1986)
11. G. Carelli, N. Ioli, A. Moretti, D. Pereira, F. Strumia: *Appl. Phys. B* **44**, 111 (1987)
12. R.J. Saykally, K.M. Evenson, D.A. Jennings, L.R. Zink, A. Scalabrin: *Int. J. Infrared Millimeter Waves* **8**, 653 (1987)
13. R. Wessel, T. Theiler, F. Keilmann: *IEEE J. Quantum Electron.* **QE-23**, 385 (1987)
14. E.M. Telles, L.R. Zink, K.M. Evenson: *Int. J. Infrared Millimeter Waves* **19**, 1627 (1998)
15. E.C.C. Vasconcellos, S.C. Zerbetto, L.R. Zink, K.M. Evenson: *Int. J. Infrared Millimeter Waves* **21**, 477 (2000)
16. E.C.C. Vasconcellos, S.C. Zerbetto, J.C. Holecek, K.M. Evenson: *Opt. Lett.* **20**, 1392 (1995)
17. E.M. Telles, H. Odashima, L.R. Zink, K.M. Evenson: *J. Mol. Spectrosc.* **195**, 360 (1999)
18. F.R. Petersen, K.M. Evenson, D.A. Jennings, J.S. Wells, K. Goto, T.J. Bridges: *IEEE J. Quantum Electron.* **11**, 838 (1975)
19. D.T. Hodges: *Infrared Phys.* **18**, 375 (1978)
20. E.M. Telles, L.R. Zink, K.M. Evenson: *J. Mol. Spectrosc.* **191**, 206 (1998)
21. M. Inguscio, L.R. Zink, K.M. Evenson, D.A. Jennings: *IEEE J. Quantum Electron.* **26**, 575 (1990)
22. J.C.S. Moraes: *J. Mol. Spectrosc.* **185**, 325 (1997)
23. G. Moruzzi, B.P. Winnewisser, M. Winnewisser, I. Mukhopadhyay, F. Strumia: *Microwave, Infrared, and Laser Transitions of Methanol: Atlas of Assigned Lines from 0 to 1258 cm⁻¹* (CRC, Boca Raton 1995)